

# Persistent *Salmonella enterica* Serovar Typhimurium Infection Induces Protease Expression During Intestinal Fibrosis

Katrin Ehrhardt, PhD,<sup>\*a</sup> Natalie Steck, PhD,<sup>†a</sup> Reinhild Kappelhoff, PhD,<sup>‡</sup> Stephanie Stein, MSc,<sup>†b</sup> Florian Rieder, MD,<sup>§</sup> Ilyssa O. Gordon, MD, PhD,<sup>¶</sup> Erin C. Boyle, PhD,<sup>||,\*\*</sup> Peter Braubach, MD,<sup>††</sup> Christopher M. Overall, PhD,<sup>‡‡</sup> B. Brett Finlay, PhD,<sup>‡‡</sup> and Guntram A. Grassl, PhD<sup>\*c</sup>

**Background:** Intestinal fibrosis is a common and serious complication of Crohn's disease characterized by the accumulation of fibroblasts, deposition of extracellular matrix, and formation of scar tissue. Although many factors including cytokines and proteases contribute to the development of intestinal fibrosis, the initiating mechanisms and the complex interplay between these factors remain unclear.

**Methods:** Chronic infection of mice with *Salmonella enterica* serovar Typhimurium was used to induce intestinal fibrosis. A murine protease-specific CLIP-CHIP microarray analysis was employed to assess regulation of proteases and protease inhibitors. To confirm up- or downregulation during fibrosis, we performed quantitative real-time polymerase chain reaction (PCR) and immunohistochemical stainings in mouse tissue and tissue from patients with inflammatory bowel disease. In vitro infections were used to demonstrate a direct effect of bacterial infection in the regulation of proteases.

**Results:** Mice develop severe and persistent intestinal fibrosis upon chronic infection with *Salmonella enterica* serovar Typhimurium, mimicking the pathology of human disease. Microarray analyses revealed 56 up- and 40 downregulated proteases and protease inhibitors in fibrotic cecal tissue. Various matrix metalloproteases, serine proteases, cysteine proteases, and protease inhibitors were regulated in the fibrotic tissue, 22 of which were confirmed by quantitative real-time PCR. Proteases demonstrated site-specific staining patterns in intestinal fibrotic tissue from mice and in tissue from human inflammatory bowel disease patients. Finally, we show in vitro that *Salmonella* infection directly induces protease expression in macrophages and epithelial cells but not in fibroblasts.

**Conclusions:** In summary, we show that chronic *Salmonella* infection regulates proteases and protease inhibitors during tissue fibrosis in vivo and in vitro, and therefore this model is well suited to investigating the role of proteases in intestinal fibrosis.

**Key Words:** intestinal fibrosis, inflammation, proteases, *Salmonella*

## INTRODUCTION

Intestinal fibrosis is a common complication of inflammatory bowel disease (IBD), especially in Crohn's disease (CD) patients due to transmural inflammation and pathology usually affecting the entire thickness of the bowel wall.<sup>1</sup> Although many cell types (fibroblasts, smooth muscle cells, endothelial or epithelial cells) and soluble factors including cytokines, growth factors, and proteases have been identified to be involved in intestinal fibrosis, the initiating mechanisms and the

complex interplay between these factors during disease development remain elusive.<sup>2</sup>

Proteases in the intestine are produced by various cell types and fulfill a number of important functions in health and disease, including tissue remodeling, nutrient digestion, modulating intestinal barrier function, activating signaling cascades, and modulating host defense to infections.<sup>3, 4</sup> Proteases can be classified as metallo-, aspartic, cysteine, serine, and threonine proteases, depending on the nature of the functional group at their active sites. The family of

Received for publications June 19, 2018; Editorial Decision March 22, 2019.

From the <sup>a</sup>Institute of Medical Microbiology and Hospital Epidemiology and German Center for Infection Research (DZIF), Partner Site Hannover, Hannover Medical School, Hannover, Germany; <sup>†</sup>Institute for Experimental Medicine, Christian-Albrechts University of Kiel, Kiel, Germany, and Research Center Borstel, Borstel, Germany; <sup>‡</sup>Department of Oral Biological and Medical Sciences, Centre for Blood Research, Faculty of Dentistry, University of British Columbia, Vancouver, BC, Canada; <sup>§</sup>Department of Gastroenterology, Hepatology and Nutrition, Digestive Diseases and Surgery Institute, and <sup>¶</sup>Department of Pathology, Pathology and Laboratory Medicine Institute, Cleveland Clinic Foundation, Cleveland, Ohio, USA; <sup>||</sup>Department of Cardiothoracic, Transplantation, and Vascular Surgery, <sup>\*\*</sup>Institute for Laboratory Animal Science and <sup>††</sup>Institute for Pathology, Hannover Medical School, Hannover, Germany; <sup>‡‡</sup>Michael Smith Laboratories, University of British Columbia, Vancouver, BC, Canada

<sup>\*</sup>Equal contribution

<sup>b</sup>Present affiliation: Center for Internal Medicine, I. Medical Clinic and Polyclinic, University Medical Center Hamburg-Eppendorf, Hamburg, Germany

Supported by: This work was funded by DFG Collaborative Research Center SFB 900 TP8 to G.A.G. Work in the lab was also supported by the DFG Priority Program SPP1656/2 and Infect-ERA Consortium Grant 031L0093B (G.A.G.) and the Canadian Academy of Health Sciences Foundation Grant 148408 (C.M.O.).

Address correspondence to: Guntram A. Grassl, PhD, Institute of Medical Microbiology and Hospital Epidemiology, Hannover Medical School, Carl-Neuberg-Str. 1, 30625 Hannover, Germany ([grassl.guntram@mh-hannover.de](mailto:grassl.guntram@mh-hannover.de)).

© 2019 Crohn's & Colitis Foundation. Published by Oxford University Press on behalf of Crohn's & Colitis Foundation.

This is an Open Access article distributed under the terms of the Creative Commons Attribution Non-Commercial License (<http://creativecommons.org/licenses/by-nc/4.0/>), which permits non-commercial re-use, distribution, and reproduction in any medium, provided the original work is properly cited. For commercial re-use, please contact [journals.permissions@oup.com](mailto:journals.permissions@oup.com)

doi: 10.1093/ibd/izz070

Published online 8 May 2019

matrix metalloproteinases (MMPs) comprises 23 members in humans and mice and is divided into subfamilies according to their domain structure: collagenases, gelatinases, stromelysins, matrilysins, elastases, membrane-type MMPs, and others.<sup>5</sup> MMPs act like “molecular scissors,” with their primary substrates being extracellular matrix (ECM) components such as collagens, laminins, fibronectins, and elastins; however, many more substrates including cytokines, chemokines, membrane receptors, and antimicrobial peptides have recently been identified.<sup>6</sup> To prevent excessive proteolytic activity and tissue damage, protease synthesis, storage, and activity are tightly controlled. For example, MMPs are activated by proteolytic cleavage, and their activity is controlled by specific tissue inhibitors of metalloproteinases (TIMPs) and by nonspecific inhibitors (eg,  $\alpha$ 2-macroglobulin).<sup>7</sup> Aberrant expression and/or activity of MMPs have been reported in several pathologies including cardiovascular diseases, obesity, type II diabetes,<sup>8</sup> cancer, IBD, and fibrosis.<sup>9,10</sup> With regard to intestinal fibrosis, dysregulation of MMPs is thought to play a crucial role in the massive remodeling and excessive collagen accumulation that occurs within the intestinal wall.<sup>11</sup> Dysregulation of MMPs and its inhibitors is in part due to the aberrant production of transforming growth factor- $\beta$  (TGF- $\beta$ ) during fibrosis.<sup>12</sup> Recently, it was shown that inhibition of MMP9 ameliorates intestinal fibrosis in a heterotopic intestinal transplant model.<sup>13</sup>

Little is known about the early developmental stages of intestinal fibrosis. Various animal models are available for IBD; however, very few can be used to study fibrogenic processes in the intestine.<sup>14</sup> Previously, we described characteristics of chronic colitis and intestinal fibrosis in *Salmonella enterica* serovar Typhimurium (*S. Typhimurium*)–infected mice, which resembled many features frequently seen in fibrotic lesions of Crohn’s disease patients.<sup>15,16</sup> In the course of persistent infection, animals develop severe transmural inflammation, accompanied by extensive type I collagen deposition and increased levels of transforming growth factor- $\beta$ 1, connective tissue growth factor, and insulin-like growth factor 1. Our studies and others have demonstrated that *S. Typhimurium*–induced colitis is a useful model to study early and progressive events in the development of intestinal fibrosis.<sup>17–19</sup> Here, we identify proteases and their inhibitors associated with the development of intestinal fibrosis by using the *S. Typhimurium*–induced colitis mouse model.

## METHODS

### Mice and Bacterial Infection

129Sv/J mice were bred in the Animal Unit at the University of British Columbia (UBC). C57Bl/6J mice were purchased from Jackson Laboratories (Bar Harbour, ME, USA) and housed at the Research Center in Borstel, Germany.

**TABLE 1. Primers Used in This Study**

Primer Name	Sequence
Cathepsin C F	CCAAGGCTTCGAGATTGTGT
Cathepsin C R	CCACCCAGTCATGGTCTCAT
Cathepsin D F	AGCATTAGTTCTCCTCCGGG
Cathepsin D R	CCGGTCTTTGACAACCTGAT
Cathepsin K F	CGGCTATATGACCACTGCCT
Cathepsin K R	TGCCGTGGCGTTATACATAC
GAPDH F	ATTGTCAGCAATGCATCCTG
GAPDH R	ATGGACTGTGGTCATGAGCC
Granzyme K F	CTAAAACCACGGTGGGAGAG
Granzyme K R	GCAGCAAGCATATTTGTGGA
HPRT F	AGTGTGGATACAGGCCAGAC
HPRT R	CGTGATTCAAATCCCTGAAGT
Meprip beta F	TTTGGGTCTGGACCTTTTTTG
Meprip beta R	TGGTATGTGGCCATCTCTTG
klk1b5 F	TGATCCTGTTCCCTAGCCCTG
klk1b5 R	GAAGCGGTACACAGCCACTT
klk1b8 F	CTAGCCCTGTCCCTAGGAGG
klk1b8 R	CCAGGGTTGGGAATTCTTCT
klk1b22 F	CCTGATCCTGTTCCCTAACCC
klk1b22 R	CCAGGGTTGGGAATTCTTCT
MMP10 F	AGCCACAAGTTGATGCTGTG
MMP10 R	TATGTGTGTCACCGTCCTGG
MMP13 F	TGATGAAACCTGGACAAGCA
MMP13 R	GGTCCTTGAGTGATCCAGA
MMP2 F	CCAGCAAGTAGATGCTGCCT
MMP2 R	GGGGTCCATTTTCTTCTTCA
MMP3 F	CGATGATGAACGATGGACAG
MMP3 R	AGCCTTGGCTGAGTGGTAGA
MMP7 F	AGTTTTCCAGTCATGGGCAG
MMP7 R	CACATCAGTGGGAACAGGC
MMP8 F	CGCCTGAAGACACTTCCATT
MMP8 R	CCGGAATTGATTGCTTGGTA
PAR-1 F	AGGGGGACCAGTTCAAATGT
PAR-1 R	GTCCCTATGAGCCAGCCAG
PAR-2 F	GTTCTACCGGAACCCCTTTC
PAR-2 R	TGGGAGGTATCACCCCTTCTG
PAR-4 F	CACTGTCGTTGGCACAGAAT
PAR-4 R	AGAGAGTACCAGGGGAAGCC
Serpina3m F	GGAGTCAGCTATCACAGAGGC
Serpina3m R	TCTGAGAAGCAGAGGACGGT
Stefin A1 F	AACCTGCCACACCAGAAATC
Stefin A1 R	CTCAACGGCTTCGAATTTTT
Timp-1 F	ATCTGGCATCCTCTTGTTCG
Timp-1 R	TGGGGAACCCATGAATTTAG
Tryptase g F	GTGGTCTGACTCTGCTGTG
Tryptase g R	GAGTTTGAAACCTGGGGATG

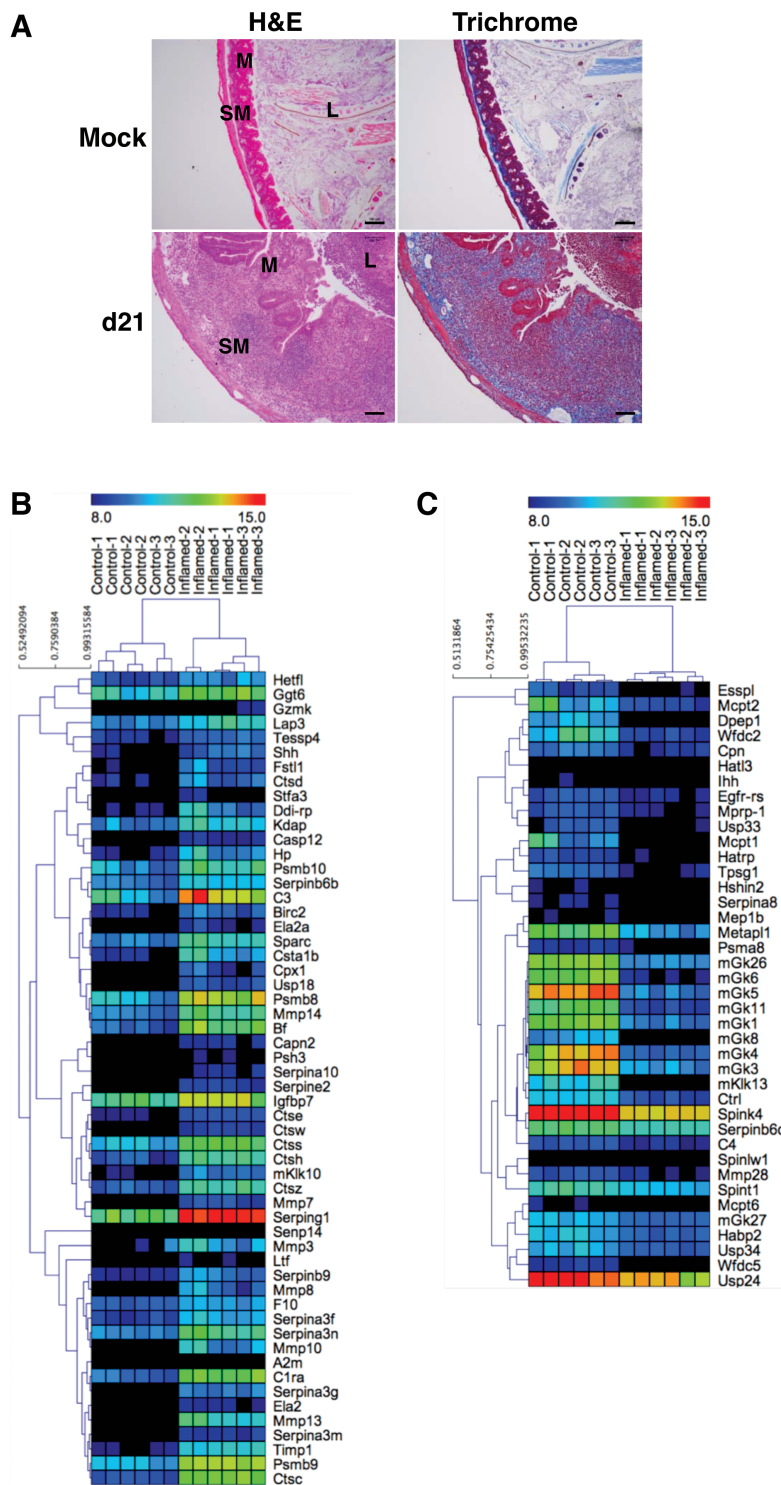


FIGURE 1. Chronic *Salmonella* infection in mice induces expression of proteases and their inhibitors. 129SvJ mice were treated with streptomycin and 24 hours later infected with *Salmonella* Typhimurium. Twenty-one days post-infection, the mice were killed and their tissues collected. A, Histopathological changes in chronically inflamed ceca (hematoxylin and eosin staining). ECM deposition is apparent in the submucosa and mucosa of infected mice, as visualized by Masson's Trichrome staining. Abbreviations: L, lumen; M, mucosa; SM, submucosa. B, Significance analysis for microarrays with hierarchical cluster analysis using a Pearson correlation average linkage method revealed 56 upregulated and (C) 40 downregulated proteases and inhibitor gene transcripts in the fibrotic cecum in comparison with the control cecum on murine CLIP-CHIP microarray.

*S. Typhimurium* SL1344<sup>20</sup> and *S. Typhimurium* SL1344  $\Delta$ *aroA*<sup>15</sup> were grown overnight in Luria-Bertani broth at 37°C with shaking. At an age of 8–12 weeks, mice were given 20 mg of streptomycin by oral gavage 24 hours before infection by oral gavage with  $3 \times 10^6$  *S. Typhimurium* suspended in 100  $\mu$ L of HEPES buffer (100 mmol/L, pH 8.0).

## Ethics Statement

All experiments were conducted in accordance with the ethical requirements and approval of the Animal Care Committee at UBC and of the Animal Care Committee of the Ministry of Energy, Agriculture, the Environment and Rural Areas of Schleswig-Holstein, Germany, and in direct accordance with the German Animal Protection Law. The protocols were approved by the Ministry of Energy, Agriculture, the Environment and Rural Areas of Schleswig-Holstein, Germany (Protocol#: V244-7224.121.3). Approval for the use of human tissue samples was obtained by the Institutional Review Board of the Cleveland Clinic, Ohio. Tissue samples were collected from CD and UC patients or from non-inflamed tissue samples from non-IBD patients.

## Cell Culture and In Vitro Infections

NIH 3T3 mouse fibroblasts were grown in DMEM containing 10% newborn calf serum. Mode-K mouse intestinal epithelial cells were grown in DMEM containing 10% fetal calf serum (FCS) and 1% 4-(2-hydroxyethyl)-1-piperazineethanesulfonic acid (HEPES). To obtain primary bone marrow-derived macrophages (BMDM), the bone marrow from mouse femurs and tibia was flushed out with phosphate buffered saline (PBS), and the cells were differentiated in Dulbecco's Modified Eagle's Medium (DMEM) containing 10% FCS, penicillin (100 U/mL), streptomycin (100  $\mu$ g/mL), 1% HEPES, and 50 ng/mL of macrophage colony-stimulating factor (M-CSF). After 1 day, macrophage progenitors were separated from the adherent fibroblasts. BMDM were cultured for another 6 days before infection. All cells were cultured at 37°C in a humidified atmosphere with 5% CO<sub>2</sub>. One day before infection, cells were seeded into 24-well plates in their respective medium without antibiotics. Bacteria were grown overnight in Luria-Bertani broth at 37°C with shaking, diluted 1:30, and grown to mid-logarithmic phase. Fibroblasts and BMDM were infected with *S. Typhimurium* at a multiplicity of infection (MOI) of 10, and Mode-K cells were infected with an MOI of 50. Gentamicin protection assays were performed as previously described.<sup>21</sup>

## Murine CLIP-CHIP Microarray Analysis

The murine CLIP-CHIP is a custom DNA microarray that covers all murine proteases, inactive homologues, and their inhibitors.<sup>22</sup> The murine CLIP-CHIP contains 70-mer oligonucleotides for 27 aspartic, 158 cysteine, 204 metallo-

221 serine, and 26 threonine proteases, along with 187 protease inhibitor gene transcripts. Each glass slide contains 2 copies of the CLIP-CHIP microarray that can be used as a technical replicate for statistical analysis. Apart from protease and protease inhibitor oligonucleotides, the microarray also contains positive and negative control oligonucleotides.

Total RNA was isolated from cecal tissues using the RNeasy-Mini Kit with an on-column DNaseI treatment (Qiagen, Mississauga, ON, Canada). The CLIP-CHIP microarray sample preparation was conducted as described in Kappelhoff et al.<sup>22</sup> and Kappelhoff and Overall.<sup>23</sup> In brief, using the Message Amp II kit (Ambion, Austin, TX, USA), 1  $\mu$ g of total RNA was reversed-transcribed into cDNA. Second-strand synthesis was performed using DNA polymerase. Purified dsDNA was used for linear amplification of amplified RNA (aRNA) by the T7 RNA polymerase.

Using the universal linking system (ULS) aRNA labeling kit (Kreatech, Amsterdam, the Netherlands), 2  $\mu$ g of aRNA (from control or fibrotic tissue) was labeled with Cy5-ULS, and a universal reference RNA was labeled with Cy3-ULS. Experimental and reference RNAs were then pooled and hybridized to a murine CLIP-CHIP microarray.

Microarray scanning and image and data analyses were done as described in Kappelhoff et al.<sup>24</sup> In brief, after stringent washes, the CLIP-CHIP microarrays were scanned using the 428 Array Scanner (MWG), and images were analyzed using ImaGene6.1 Software (Biodiscovery). CarmaWEB software was used to normalize the data, and MeV from the TM4 Microarray Suite ([www.tigr.org](http://www.tigr.org)) was used for statistical analysis. Significance analysis for microarrays (SAM) was performed according to Tusher et al.<sup>25</sup> using 924 unique permutations in a 2-class unpaired analysis with a delta value of 2.254 for a false discovery rate of 0%. SAM was used to find significant changes in expression of proteases and protease inhibitors. The hierarchical cluster analysis of significant genes was done using Pearson correlation with a complete linkage method in MeV.

## Quantitative Real-time Polymerase Chain Reaction

RNA was extracted from mouse cecal tissue using the High Pure RNA Tissue Kit (Roche). RNA was reverse-transcribed into cDNA using the cDNA Synthesis Kit (Roche) according to the manufacturer's instructions. Quantitative real-time PCR (qPCR) was performed with SYBR-Green Mastermix (Roche) and gene-specific primers (Table 1). Data were normalized to house-keeping genes *Gapdh* and *Hprt1*, and fold regulation was calculated using the  $\Delta\Delta C_t$  method.

## Immunohistochemistry

Formalin-fixed, paraffin-embedded tissue sections were deparaffinized and rehydrated. Samples included cecum tissue from uninfected (n = 5) and infected (n = 5) mice and human

**TABLE 2.** Significantly Upregulated Protease and Protease Inhibitor Transcripts Detected With the Murine CLIP-CHIP During *Salmonella*-Induced Fibrosis

Merops ID	Description	Gene	RefSeq_1	Fold Change
M10.006	stromelysin 2	Mmp10	NM_019471	21.99
M10.013	collagenase 3	Mmp13	NM_008607	12.85
C01.070	cathepsin C	Ctsc	NM_009982	11.43
M10.002	collagenase 2	Mmp8	NM_008611	10.62
I04.xxx	a1-antitrypsin member 3g	Serpina3g	XM_484175	10.17
S01.196	complement factor B	Bf	NM_008198	8.03
S01.192	complement component C1ra	C1ra	NM_023143	7.65
I39.950ni	complement component 3	C3	NM_009778	7.15
I35.001	tissue inhibitor of metalloprotease-1	Timp1	NM_011593	6.73
T01.013	proteasome catalytic subunit 1i	Psmb9	NM_013585	6.28
T01.015	proteasome catalytic subunit 3i	Psmb8	NM_010724	6.25
I04.024	C1 inhibitor	Serping1	NM_009776	6.09
C01.040	cathepsin H	Ctsh	NM_007801	5.28
M14.015np	carboxypeptidase X1	Cpx1	NM_019696	5.15
I25.xxx	stefin-2 like	Csta1b	NM_173869	5.02
S01.972np	haptoglobin-1	Hp	NM_017370	4.79
A02.059	DDI-related protease	Ddi-rp	NM_026414	4.77
I04.xxx	a1-antitrypsin member 3m	Serpina3m	NM_009253	4.42
S60.001	lactotransferrin	Ltf	NM_008522	4.40
C01.013	cathepsin Z	Ctsz	NM_022325	4.22
C46.002	sonic hedgehog protein	Shh	NM_009170	4.02
I25.xxx	stefin A3	Stfa3	NM_025288	3.79
S01.155	pancreatic elastase II (IIA)	Ela2a	NM_015779	3.79
C01.037	cathepsin W	Ctsw	NM_009985	3.73
M10.005	stromelysin 1	Mmp3	NM_010809	3.72
S01.246	kallikrein hK10	mKlk10	NM_133712	3.69
I04.xxx	a1-antitrypsin member 3n	Serpina3n	NM_009252	3.68
C19.030	USP18	Usp18	NM_011909	3.64
M10.014	MT1-MMP	Mmp14	NM_008608	3.49
I04.005	protein Z-dependent PI	Serpina10	NM_144834	3.38
C01.034	cathepsin S	Ctss	NM_021281	3.37
I01.xxx	folliculin-like 1	Fstl1	NM_008047	3.37
C48.xxx	sentrin/SUMO protease 14	Senp14	BN000389	3.32
S01.146	granzyme K	Gzmk	NM_008196	3.19
I04.xxx	a1-antitrypsin member 3f	Serpina3f	BC049975	3.12
M10.008	matrilysin	Mmp7	NM_010810	3.02
I39.001	a-2-macroglobulin	A2m	NM_175628	3.00
A01.009	cathepsin D	Ctsd	NM_009983	2.99
S01.131	neutrophil elastase	Ela2	NM_015779	2.96
I01.xxx	folliculin-like 2/IGFBP7	Igfbp7	NM_008048	2.92
I04.014	protease inhibitor 9/CAP3	Serpib9	NM_009256	2.80
I01.xxx	osteonectin	Sparc	NM_009242	2.76
T01.014	proteasome catalytic subunit 2i	Psmb10	NM_013640	2.67
C14.013	caspase-12	Casp12	NM_009808	2.53
T03.022	gamma-glutamyltransferase 6	Ggt6	NM_027819	2.49
I32.003	cIAP2	Birc2	NM_007464	2.32
M17.001	leucyl aminopeptidase	Lap3	NM_024434	2.31

TABLE 2. Continued

Merops ID	Description	Gene	RefSeq_1	Fold Change
A01.046	napsin A	Kdap	NM_008437	2.28
A01.010	cathepsin E	Ctse	NM_007799	2.20
Cx1.xxxxnp	HetF-like	Hetfl	NM_024477	2.04
S01.099	testis serine protease 4	Tessp4	NM_199471	1.94
A22.003	presenilin homolog 3/SPP	Psh3	NM_010376	1.91
C02.002	calpain 2	Capn2	NM_009794	1.90
I04.021	proteinase nexin 1/GDN	Serpine2	NM_009255	1.90
I04.xxx	protease inhibitor 6b	Serpinb6b	NM_011454	1.86
S01.216	coagulation factor Xa	F10	NM_007972	1.86

The letter in front of a number refers to the protease class (A, aspartic protease; C, cysteine protease; M, metalloprotease; S, serine protease; T, threonine protease; I, protease inhibitor).

colon samples from non-IBD (n = 5), UC (n = 5), or CD (n = 5) patients. Antigen unmasking was achieved by heat treatment in 10 mM of sodium citrate buffer (pH 6.0) or Tris-EDTA buffer (pH 9.0) for 30 minutes. Specimens were incubated with blocking reagent containing 1% bovine serum albumin, 0.1% Triton X-100, 0.05% Tween 20, and 2% normal goat serum. Antigen retrieval, primary antibodies, and dilutions are listed in [Supplementary Table 1](#). Horseradish peroxidase-labeled secondary antibodies were used and were followed by incubation with 3,3'-Diaminobenzidine (DAB) substrate. Negative controls were done by omission of the primary antibody. The pattern (focal, patchy, or diffuse) and intensity (0–3) of antibody staining were analyzed in the epithelium, lamina propria, submucosa, and muscularis propria. Representative images are shown and were obtained using an Olympus BX41 microscope.

## Statistics

Statistical analysis of qPCR and bacterial colonization data was performed using the GraphPad Prism 5 software package (GraphPad Software, San Diego, CA, USA). One-way analysis of variance (ANOVA) and Tukey's multiple comparison tests were used to determine significance between multiple data sets. The Student *t* test was used to compare two groups. A *P* value <0.05 was considered statistically significant.

## RESULTS

### Salmonella-Induced Intestinal Fibrosis in Mice Is Linked to the Differential Regulation of Multiple Proteases

We have previously shown that long-term infection with *S. Typhimurium* leads to chronic inflammation and the development of fibrosis in the cecum and colon of mice.<sup>15</sup> 129Sv/J mice infected with wild-type *S. Typhimurium* developed persistent fibrosis in the cecum, peaking 21 days postinfection. At this

time point, ceca were inflamed and fibrotic. Crypt architecture was destroyed, and the mucosa, submucosa, and muscularis were infiltrated with large amounts of inflammatory cells and fibroblasts. In addition, collagen was deposited in the mucosa and submucosa, as visualized by Masson's Trichrome staining ([Fig. 1A](#)). Microarray analysis on cecal tissue was performed to identify proteases and protease inhibitors regulated during chronic inflammation and fibrosis. We used the murine CLIP-CHIP degradome microarray, which is a dedicated and focused array that allows analysis of all 636 proteases and 187 protease inhibitor gene transcripts in the murine genome at the mRNA transcript level.<sup>22</sup>

Significance analysis for microarrays of the microarray data revealed 96 significantly regulated proteases and inhibitors. Fifty-six genes were upregulated and 40 genes were downregulated in fibrotic cecal tissue when compared with normal control tissue from mock-infected mice ([Fig. 1B, C](#), [Table 2](#), [Table 3](#); see [Supplementary Data Table S2](#) for a complete list of CLIP-CHIP results).

The differential expression of proteases and protease inhibitors was further confirmed by qPCR analysis. Some of the most strongly upregulated proteases were from the MMP family. Expression of *Mmp3*, *Mmp7*, *Mmp8*, *Mmp10*, and *Mmp13* was strongly increased in fibrotic cecal tissue 21 days post-infection ([Fig. 2A](#)). In contrast, expression of *Mmp2* did not change during infection. Of note, the epithelial barrier-promoting metalloprotease meprin- $\beta$  (*Mep1b*) was significantly downregulated in fibrotic tissue. As depicted in [Figure 2B](#), expression of glandular kallikreins *Klk1b5*, *Klk1b8*, and *Klk1b22* and tryptase- $\gamma$  (*Tpsg1*) was significantly decreased, whereas expression of granzyme K (*Gzmk*) increased upon fibrosis development. The induction of several cathepsins (*Ctsc*, *Ctsd*, *Ctsk*) was confirmed by our qPCR results ([Fig. 2C](#)). Various protease inhibitors including *Serpina3m* and stefinA1 (*Stfal*), along with the tissue inhibitor of metalloproteases-1 (*Timp1*), were also

**TABLE 3.** Significantly Downregulated Protease and Protease Inhibitor Transcripts Detected With the Murine CLIP-CHIP During *Salmonella*-Induced Fibrosis

Merops ID	Description	Gene	RefSeq_1	Fold Change
S01.037	glandular kallikrein mK5	mGk5	NM_008456	-19.49
S01.xxx	glandular kallikrein mK6	mGk6	NM_010639	-18.74
S01.066np	glandular kallikrein mK4	mGk4	NM_010915	-17.74
S01.067	glandular kallikrein mK8	mGk8	NM_008457	-12.53
S01.306	kallikrein hK13	mKlk13	NM_010115	-12.51
S01.170	glandular kallikrein mK3	mGk3	NM_008693	-10.87
S01.141	mast cell protease 1	Mcpt1	NM_008570	-10.34
S01.041	glandular kallikrein mK11	mGk11	NM_010640	-8.81
S01.164	glandular kallikrein mK1	mGk1	NM_010645	-7.36
S01.070	glandular kallikrein mK26	mGk26	NM_010644	-6.93
M19.001	membrane dipeptidase	Dpep1	NM_007876	-5.73
I17.xxx	WAP four-disulfide core 2	Wfdc2	NM_026323	-4.84
S01.003	mast cell protease 2	Mcpt2	NM_008571	-4.66
M24.028	methionyl aminopeptidase-like 1	Metapl1	NM_025633	-4.41
C46.003	indian hedgehog protein	Ihh	NM_010544	-3.78
M12.004	mepirin beta subunit	Mep1b	NM_008586	-3.40
S01.256	chymopasin	Ctrl	NM_023182	-3.18
S01.028	tryptase gamma 1	Tpsg1	NM_012034	-3.07
I01.xxxni	serine PI Kazal type 4	Spink4	NM_011463	-2.88
C64.xxx	Hin-2	Hshin2	XM_358202	-2.46
C19.037	VDU1	Usp33	NM_133247	-2.45
S01.325	epidermis-specific SP-like	Esspl	BN000135	-2.33
C19.047	USP24	Usp24	XM_131566	-2.29
S01.291	HAT-related protease	Hatrp	NM_183109	-2.28
M14.004	carboxypeptidase N	Cpn	NM_030703	-2.21
I17.xxx	WAP four-disulfide core 5	Wfdc5	NM_145369	-2.21
S01.033	hyaluronan-binding ser-protease	Habp2	NM_146101	-2.17
I02.xxx	eppin	Spinlw1	NM_029325	-2.13
S01.294	HAT-like 3	Hat13	NM_001030297	-2.12
I04.953ni	angiotensinogen/AGT	Serpina8	NM_007428	-2.10
C19.067	USP34	Usp34	XM_483996	-2.09
M48.017	metalloprotease related protein 1	Mprp-1	NM_025909	-2.06
S01.242	tryptase beta 2	Mcpt6	NM_010781	-2.02
S54.952np	EGF receptor related sequence	Egfr-rs	NM_010117	-1.93
S01.073	glandular kallikrein mK27	mGk27	NM_020268	-1.92
M10.030	epilysin	Mmp28	NM_080453	-1.82
I02.007	HGF activator inhibitor 1	Spint1	NM_016907	-1.81
T01.978np	proteasome alpha 8 subunit	Psma8	AK010717	-1.78
I39.951ni	complement component 4	C4	NM_009780	-1.70
I04.xxx	protease inhibitor 6d	Serpib6d	XM_111521	-1.60

The letter in front of a number refers to the protease class (A, aspartic protease; C, cysteine protease; M, metalloprotease; S, serine protease; T, threonine protease; I, protease inhibitor).

confirmed to be upregulated (Fig. 2D) during *S. Typhimurium*-induced intestinal fibrosis. Taken together, our analysis indicated an enhanced expression of MMPs and an impairment of serine protease expression.

### Proteases Are Expressed by Epithelial Cells and Infiltrating Cells During Inflammation and Fibrosis

Next, we tested whether the gene expression changes we observed with the microarray and by qPCR can also be observed at

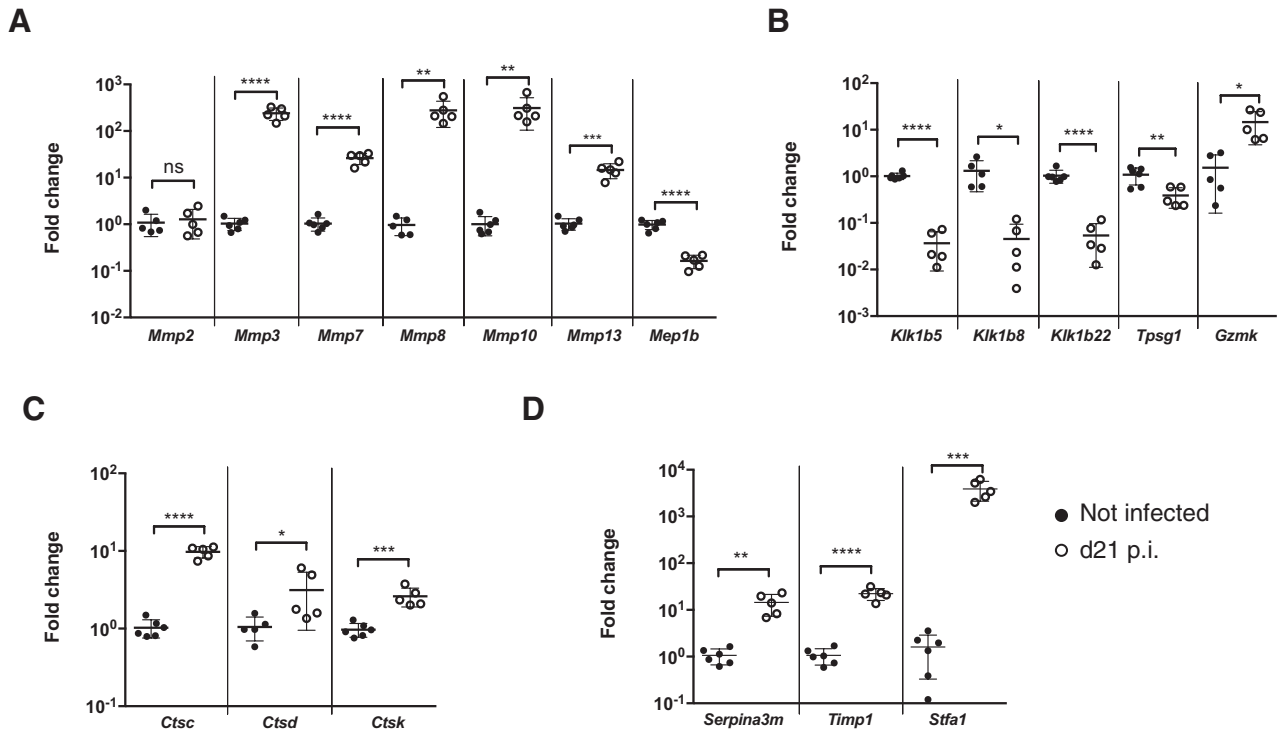


FIGURE 2. Verification of protease, protease inhibitor, and protease-activated receptor (PAR) regulation in ceca by quantitative real-time PCR 21 days post-infection. A, Metalloproteases: *Mmp3*, *Mmp7*, *Mmp8*, *Mmp10*, and *Mmp13* are upregulated, *Mep1b* (meprin- $\beta$ ) is downregulated, and *Mmp2* expression is unchanged. B, Serine proteases glandular kallikreins (*Klik1b5*, *Klik1b8*, *Klik1b22*) and *Tpsg1* (trypsin- $\gamma$ ) are downregulated, and *Gzmk* (granzyme-K) is upregulated in the fibrotic cecum. C, Cysteine proteases cathepsin C and K (*Ctsc* and *Ctsk*) and the aspartic protease cathepsin D (*Ctsd*) are upregulated in fibrotic cecum. D, Protease inhibitors *Serpina3m*, *Timp1* (tissue inhibitor of metalloproteinase 1), and *Sfta1* (stefin A1) are upregulated in the fibrotic cecum. Data are given for each mouse, including mean  $\pm$  SD ( $n = 5$  animals per group). Statistical significance was analyzed using the Student *t* test. \* $P < 0.05$ ; \*\* $P < 0.01$ ; \*\*\* $P < 0.001$ ; \*\*\*\* $P < 0.0001$ .

the protein level. Antibody staining of tissues from mock-infected and chronically infected mice demonstrate that MMP3 is weakly and MMP8 is strongly expressed in the uninfected cecum epithelium and upregulated upon *S. Typhimurium*-induced fibrosis in the cecum epithelium and infiltrating cells (Fig. 3). Positive staining for MMP7, MMP10, MMP13, cathepsin D, and granzyme K is not observed in uninfected ceca; however, in infected fibrotic tissue, MMP13 and cathepsin D are found in the inflammatory infiltrate, MMP7 is upregulated in the epithelium, and MMP10 and granzyme K are seen in both the inflammatory infiltrate and the epithelium of fibrotic tissue. Meprin- $\beta$  is strongly expressed in epithelial cells in uninfected mice. Upon experimental fibrosis, meprin- $\beta$  is downregulated and is no longer detectable by immunohistochemical staining (Fig. 3), in agreement with the microarray and qPCR data.

We next tested whether some of the proteases we see regulated in our experimental model of intestinal fibrosis are also regulated in human IBD patients (see Supplementary Tables 3 and 4 for clinical data of human subjects). Tissue sections from noninflamed controls (C) were compared with inflamed fibrotic tissue from CD and UC patients (Fig. 4A). Similar to our mouse model, the epithelium of non-inflamed controls stained positive

for MMP3 and MMP8, whereas in addition to the epithelium of CD and UC patients, there were MMP3- and MMP8-positive inflammatory cells in the lamina propria (Fig. 4B). MMP7, MMP10, and granzyme K were not detected in the noninflamed control intestines. However, in UC and CD patients, a subset of crypt epithelial cells stained strongly for MMP7. In addition, epithelial cells and inflammatory cells in IBD tissues were positive for MMP10 and granzyme K. In noninflamed control tissue, a few cells in the lamina propria were positive for cathepsin C, cathepsin D, and cystatin A. In tissues from CD patients, there was a slight increase in cathepsin C-positive cells, and there was a strong increase in cathepsin D- and cystatin A-positive cells in both CD and UC patients. Strong staining for meprin- $\beta$  and kallikrein 5 was found in the epithelium and lamina propria of all noninflamed controls, but only mild expression was detected in CD or UC patients. In noninflamed colon, we observed strong TIMP1-positive cells, which are presumably enteroendocrine cells, whereas in IBD patients other epithelial cells and some cells in the lamina propria stained positive for TIMP1 as well.

In summary, the pattern of protease staining in intestinal tissues from UC patients was very similar to that of CD



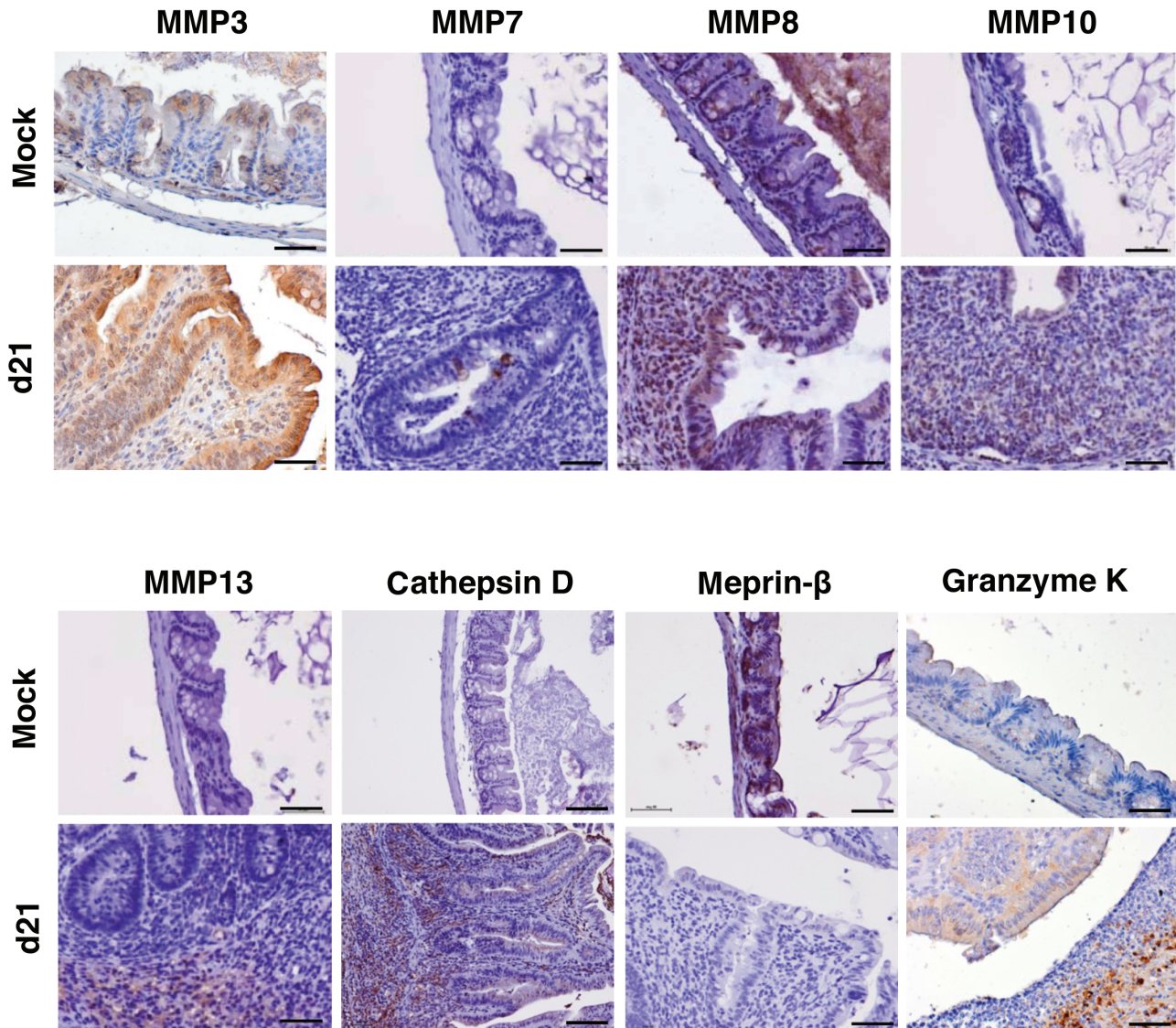


FIGURE 3. Protease expression in intestinal tissue of mice chronically infected with *S. Typhimurium*. Cecum sections of mice were stained for proteases as indicated. Original magnification 400 $\times$ ; scale bar: 50  $\mu$ m.

patients but drastically different from that of noninflamed controls. In addition, protease staining observed to be up- or downregulated in inflamed intestinal mouse tissues followed a comparable pattern in human IBD tissues.

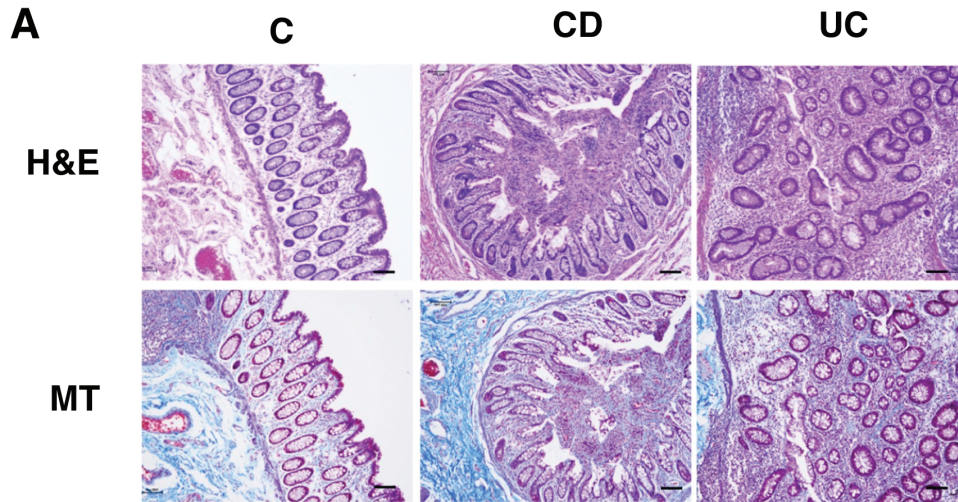
### ***Salmonella* Induces Proteases in 129SvJ and C57Bl6/J Mice to a Similar Level**

Chronic mouse infections with wild-type *S. Typhimurium* can only be performed in resistant mouse strains such as 129SvJ. However, the majority of knockout mice that would allow investigation into the contribution of specific proteases to fibrosis are generated in a *Salmonella*-sensitive C57Bl6/J background. Therefore, we infected C57Bl6/J mice with the attenuated *S. Typhimurium*  $\Delta$ *aroA* strain, which also induces chronic intestinal inflammation

and fibrosis (Fig. 5A). We analyzed the expression kinetics of selected proteases at days 7, 14, and 21 postinfection. As shown in Figure 5B, the MMPs tested were induced to a similar degree compared with 129SvJ mice infected with wild-type *Salmonella*. Therefore, C57Bl6/J mice and their gene-deficient strains can be used to study the role of specific proteases during intestinal fibrosis.

### ***Salmonella* Induces Protease Expression in Macrophages and Epithelial Cells**

We observed upregulation of specific proteases during *Salmonella*-induced chronic inflammation and fibrosis in mice. Although many cell types can express different proteases during inflammation,<sup>26</sup> the staining pattern in fibrotic mouse



Continued

and human tissue indicated specific expression patterns by epithelial cells, inflammatory cells, and fibroblasts present in the inflamed intestine. Therefore, we tested whether *in vitro* *Salmonella* infection of these cell types directly induces protease expression. Mouse primary BMDMs, fibroblasts (NIH-3T3), and epithelial cells (Mode-K) were infected with *S. Typhimurium* for up to 3 days. As shown in Figure 6, *Salmonella* invaded and persisted in all three cell types (Fig. 6A–C). Upon infection, BMDMs strongly upregulated expression of *Mmp3*, *Mmp8*, *Mmp10*, and *Mmp13* (Fig. 6D–G) but not *Mmp7* (not shown). *Salmonella* infection also induced expression of *Mmp3*, *Mmp10*, and *Mmp13* in epithelial cells (Fig. 6H–J), but not *Mmp7* or *Mmp8*. In contrast, infection of fibroblasts did not induce expression of any of the tested proteases (not shown). These data demonstrate that *S. Typhimurium* infection directly stimulates protease expression in macrophages and epithelial cells, but not in fibroblasts.

## DISCUSSION

Proteases and their inhibitors are thought to be key mediators of the intestinal fibrotic process, but their specific roles remain poorly understood. Until recently, there was a paucity of animal models to study intestinal fibrosis. The *S. Typhimurium* model is now established in the field of intestinal fibrosis as it recapitulates the pathology of human disease including transmural tissue fibrosis, a Th1/Th17 immune response, and the induction of pro-fibrotic genes. Using this model, we discovered that a plethora of proteases and protease inhibitors are regulated during intestinal fibrosis. Site-specific upregulation of several MMPs was observed, and a similar protease expression pattern was validated in human intestinal fibrotic tissue. In addition, we demonstrate that *S. Typhimurium* is capable of directly inducing expression of several proteases in a cell type-specific manner.

During intestinal fibrosis development, it is thought that tissue destruction during chronic inflammation causes an excessive healing response, leading to an imbalance between ECM deposition and ECM turnover by MMPs. Association studies show that single nucleotide polymorphisms in the stromelysin genes *MMP3* and *MMP10* are associated with an increased risk for IBD<sup>26</sup> and that the *MMP3* 5A/6A genotype is especially associated with fibro-stenosing complications and fistula formation in CD patients.<sup>27</sup> *MMP10* and *MMP13* are also described to be upregulated in the intestine of CD and UC patients.<sup>28</sup> In mice chronically infected with *Salmonella*, we observed upregulation of *Mmp3*, *Mmp10*, and *Mmp13*. At first glance, this may appear counterintuitive as MMPs have been implicated in ECM degradation, but the function of MMPs goes beyond cleavage of matrix molecules. For example, MMP3 and macrophage MMP12 can act intracellularly as transcription factors to induce pro-fibrotic connective tissue growth factor (CTGF) and IFN- $\alpha$  gene transcription, respectively.<sup>29,30</sup> MMP2, where we did not detect altered expression upon *Salmonella* infection, cleaves and inactivates CTGF, thereby unmasking VEGF.<sup>31</sup> Thus, fibrosis represents a complex inflammatory environment where the interplay of cytokines and growth factors can be orchestrated by proteases.

Although many MMPs are involved in epithelial barrier destruction, TIMP function is generally thought to be critical for epithelial barrier restitution. On the other hand, excessive TIMP expression can also result in fibrosis: *TIMP1* is upregulated in inflammatory and fibrotic lesions in patients with Crohn's disease<sup>32,33</sup> and in other mouse models of intestinal fibrosis.<sup>34</sup> In agreement with these studies, we found a strong upregulation of *Timp1* during *Salmonella*-triggered fibrosis. Besides inhibiting the action of MMPs, TIMP1 also stimulates cell proliferation and activates neutrophils.<sup>35</sup> Recently, it was shown that TIMP1-deficient mice have less fibrosis and

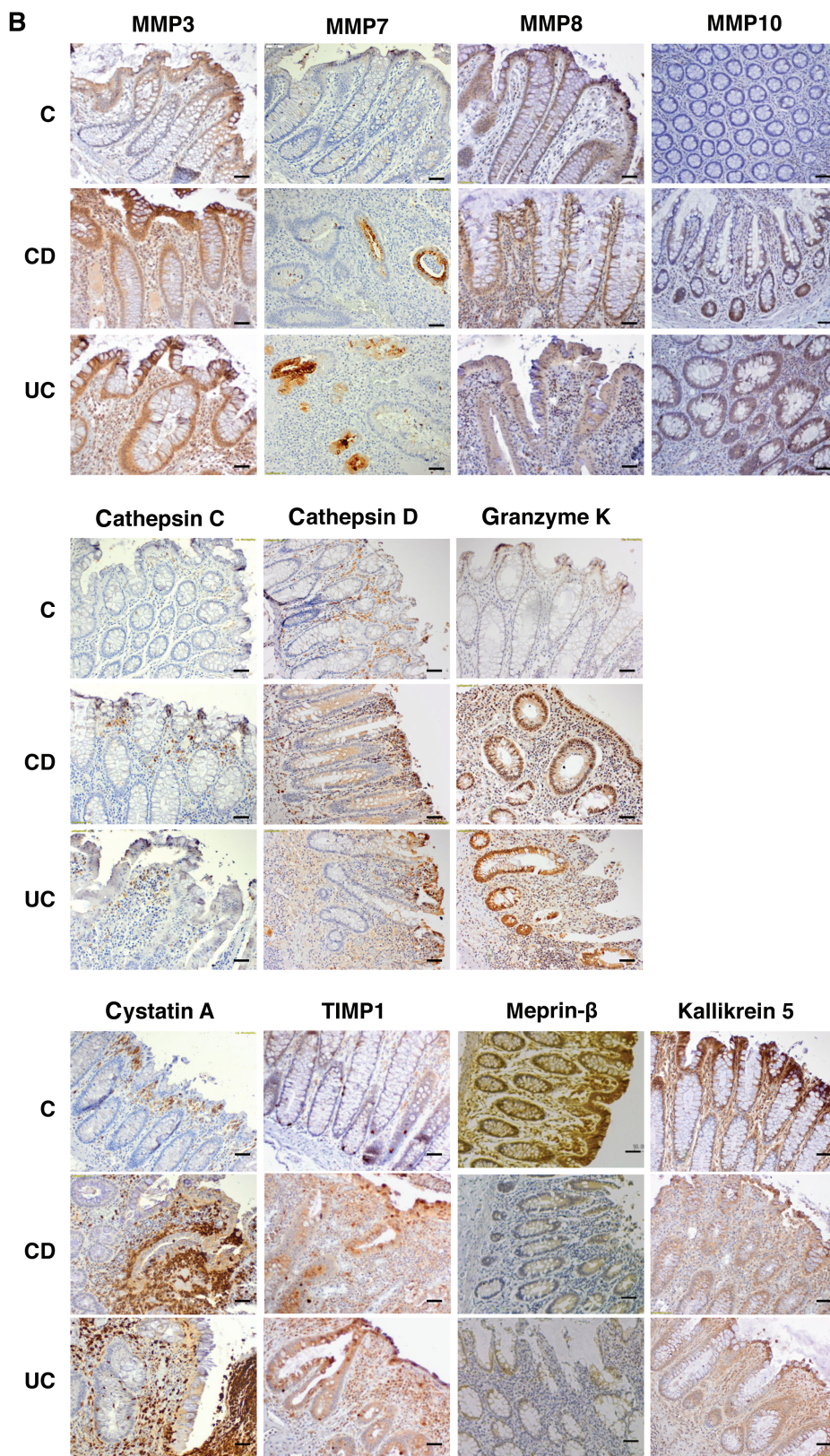


FIGURE 4. Protease expression in tissues from human IBD patients. Tissue sections were taken from Crohn's disease (CD) or ulcerative colitis (UC) patients and from non-inflamed controls (C). A, Hematoxylin and eosin and Masson's Trichrome (MT) staining showing pathological changes during disease and extracellular matrix deposition, respectively. Original magnification 100 $\times$ ; scale bar: 100  $\mu$ m. B, Protease staining. Original magnification 200 $\times$ ; scale bar: 50  $\mu$ m.

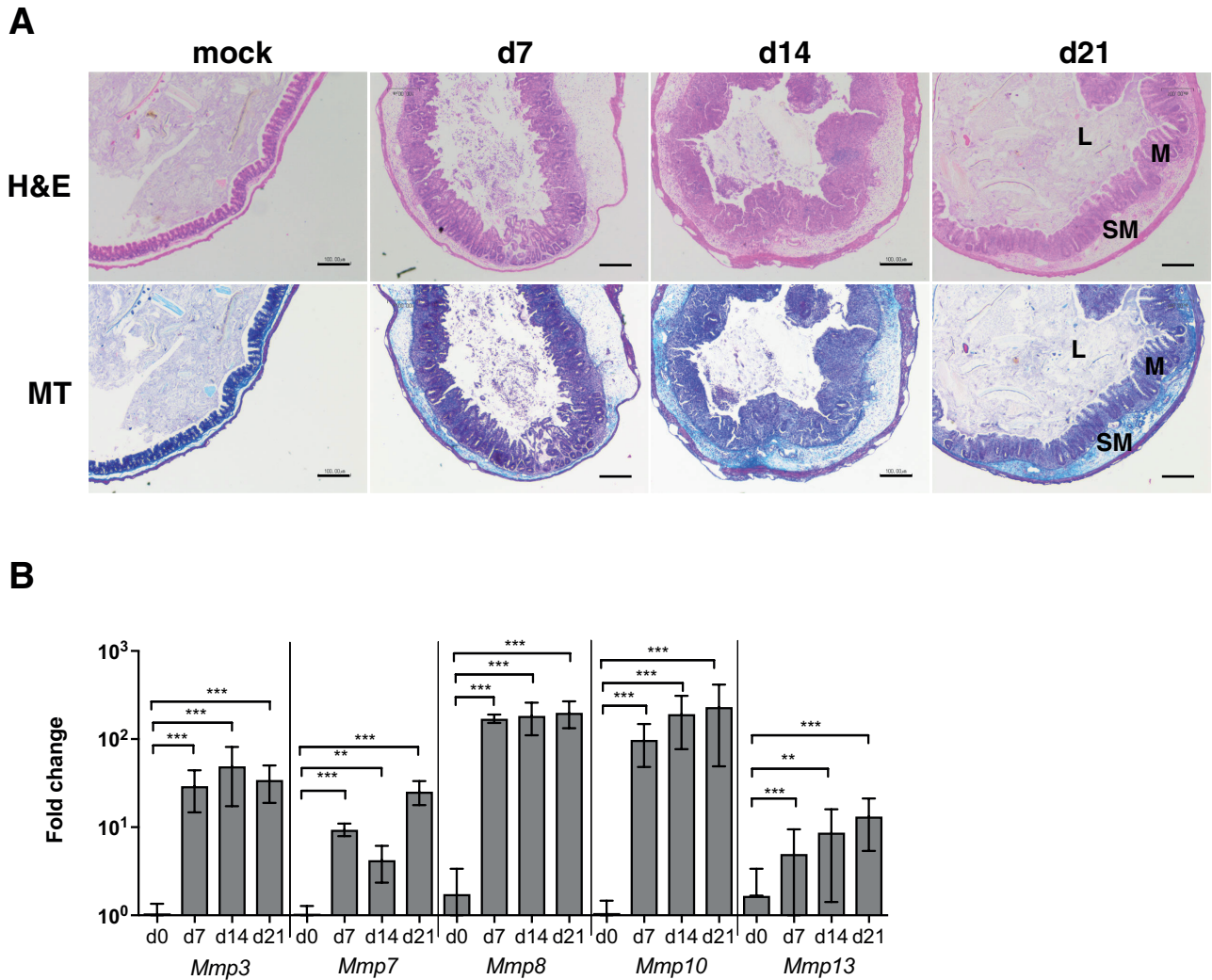


FIGURE 5. Kinetics of protease induction in *Salmonella*-infected C57Bl/6 mice. C57Bl/6 mice were treated with streptomycin and infected 24 hours later with *S. Typhimurium*  $\Delta$ aroA. Seven, 14, and 21 days postinfection, mice were killed and their tissues collected. A, Histopathological changes in chronically inflamed ceca (hematoxylin and eosin staining). ECM deposition in the submucosa and mucosa of infected mice was visualized by Masson's Trichrome (MT) staining. Abbreviations: L, lumen; M, mucosa; SM, submucosa. Scale bar: 100  $\mu$ m. B, At indicated time points, induction of proteases was assessed by qPCR. Mean values  $\pm$  SD are shown (n = 5 animals per group). Statistical significance was analyzed with 1-way ANOVA with Tukey's post-test. \*\*P < 0.01; \*\*\*P < 0.001.

inflammation upon stimulation with DSS.<sup>9</sup> Conversely, treatment of CD myofibroblasts with the anti-inflammatory drug infliximab increases TIMP1 production in a dose-dependent manner, leading to an antifibrotic effect by enhancing cell migration and decreasing collagen production.<sup>36</sup>

Meprin- $\beta$  has various roles and can lead to cytokine induction and inactivation of certain cytokines by cleavage.<sup>37</sup> Meprin- $\beta$ -deficient mice have increased amounts of pro-inflammatory cytokines and increased inflammation in a DSS colitis model.<sup>38</sup> Our data show that meprin- $\beta$  is downregulated in the fibrotic intestinal tissue of *Salmonella*-infected mice and also in IBD patient tissue, consistent with previous reports in patients.<sup>39</sup>

Various cells have been shown to be sources for proteases. In CD patients, MMP3 was seen to be produced by fibroblasts and mononuclear cells,<sup>40</sup> and MMP7 was exclusively found in enterocytes adjacent to ulcers.<sup>41</sup> In vitro, we also observed MMP3 upregulation in *Salmonella*-infected macrophages, and in chronically infected mice, MMP7 is upregulated in enterocytes. In vitro, human intestinal fibroblasts can be a major source of MMPs (MMP1, -2, -3, and -9) when stimulated with IL-21 or TNF- $\alpha$ .<sup>42</sup> However, in our experiments using a mouse fibroblast cell line infected with *S. Typhimurium*, we did not detect upregulation of *Mmp3*, *Mmp7*, *Mmp8*, *Mmp10*, or *Mmp13*. We speculate that in an in vivo setting, bacterial infection would trigger IL-21 and TNF- $\alpha$  production in other cell

types, which would then indirectly stimulate fibroblasts to produce proteases. *S. Typhimurium* infection of BMDM directly triggered upregulation of *Mmp3*, *Mmp8*, *Mmp10*, and *Mmp13*. Also to consider, many proteases are produced as inactive zymogens and need to be activated (eg, by proteolytic cleavage). Our data showing upregulation of proteases thus do not directly imply that these proteases are present in their active form.

Several MMPs have been shown to play a role in *Salmonella* infection. *Mmp2* and *Mmp9* are highly upregulated during acute *Salmonella* infection in mice, and *Mmp2/Mmp9*<sup>-/-</sup> mice are resistant to *S. Typhimurium*-induced colitis.<sup>43</sup> Furthermore, constitutive *Mmp9* expression in the intestinal

epithelium results in stronger colitis development upon acute infection with *S. Typhimurium*.<sup>44</sup> In contrast, in our chronic infection experiments, we did not detect significant changes in expression of these MMPs compared with uninfected controls, indicating that these MMPs play a role in acute but not chronic infections.

Although the etiology of IBD is still not completely understood, an aberrant response to normal microbial populations, intestinal dysbiosis, and infection with various enteric pathogens such as adherent invasive *Escherichia coli*, *Mycobacterium paratuberculosis*, *Campylobacter*, or *Salmonella* have been associated with IBD.<sup>45-48</sup> However, whether particular

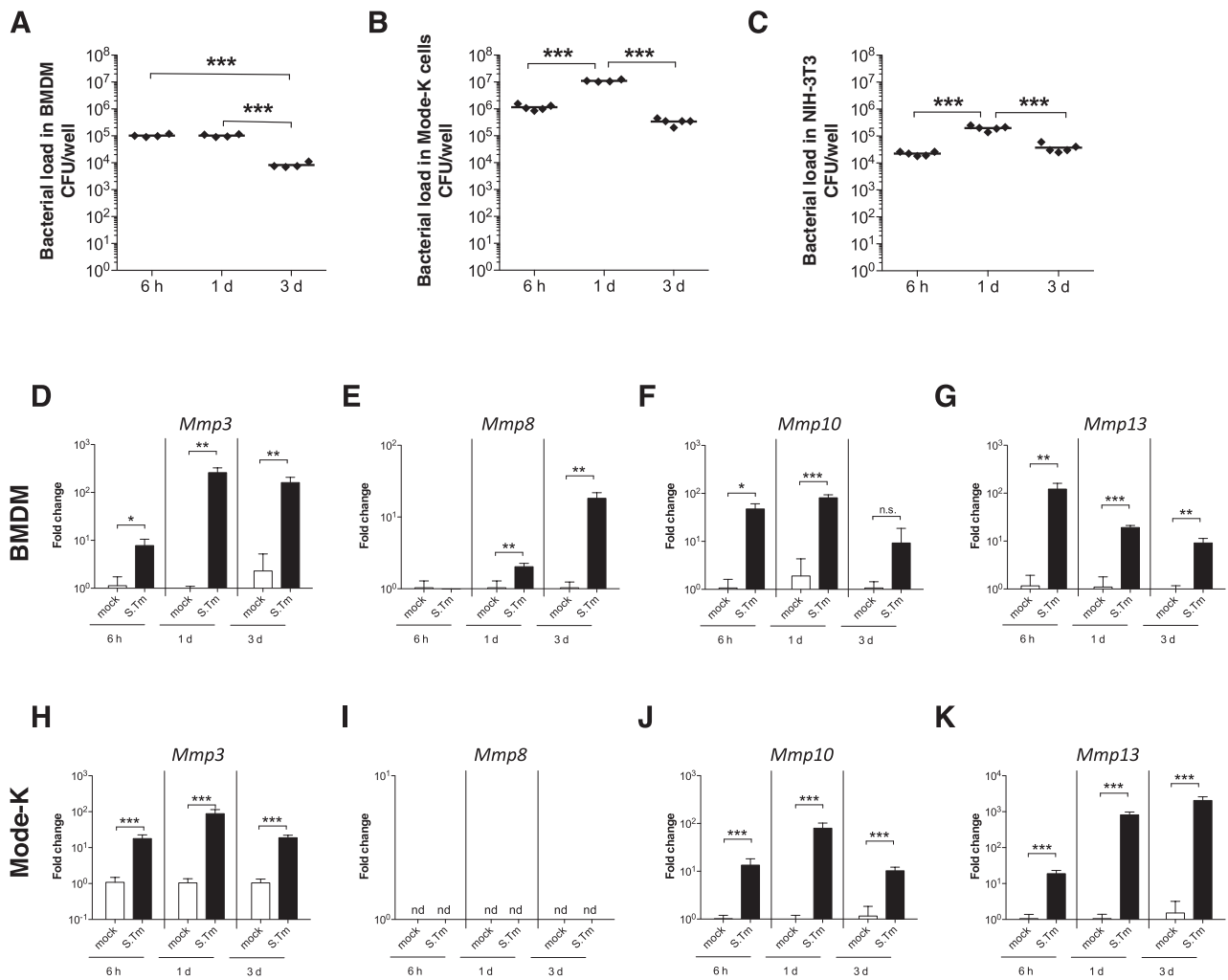


FIGURE 6. *Salmonella* infection induces protease expression in macrophages and epithelial cells. BMDMs, NIH-3T3 fibroblasts, and Mode-K epithelial cells were infected with *S. Typhimurium*. At indicated time points, cells were lysed, and intracellular bacterial counts were determined by gentamicin protection assay, demonstrating that all cell types were infected and that *Salmonella* persisted for at least 3 days inside macrophages (A), epithelial cells (B), and fibroblasts (C). Individual values and the mean +/- SD from 1 representative out of 2 independent experiments are shown (n = 4-5 per group). Statistical significance was analyzed using one-way ANOVA with Tukey's post-test. \*\*\*P < 0.001. RNA was isolated from macrophages (D-G) and epithelial cells (H-K) at the indicated time points postinfection, and protease expression was analyzed by qPCR. Individual values and the mean +/- SD from 1 representative out of 2 independent experiments are shown (n = 4-5 per group). Statistical significance was analyzed using Student's t-test. \*\*P < 0.01; \*\*\*P < 0.001.

infections cause intestinal fibrosis or whether their presence simply reflects the competitive advantage of these pathogens to expand in the inflamed gut is still under debate.<sup>49–53</sup>

To our knowledge, this is the first protease screen performed on bacterial-induced fibrosis in mice and will serve as the basis for future studies into the role of specific proteases in disease development. The *S. Typhimurium* model is now poised to provide further insight into the molecular mechanisms of bacterial-induced intestinal fibrosis. Genes regulated in the mouse model can be validated in the fibrotic tissue removed from Crohn's disease patients. In the future, specific inhibition of proteases could be a promising target for treatment of chronic inflammation and fibrosis in IBD.<sup>54</sup>

## SUPPLEMENTARY DATA

Supplementary data are available at *Inflammatory Bowel Diseases* online.

## ACKNOWLEDGMENTS

We would like to thank Katrin Seeger and Janin Braun for expert technical help.

## REFERENCES

- Spinelli A, Correale C, Szabo H, et al. Intestinal fibrosis in Crohn's disease: medical treatment or surgery? *Curr Drug Targets*. 2010;11:242–248.
- Rieder F, Fiocchi C. Intestinal fibrosis in IBD—a dynamic, multifactorial process. *Nat Rev Gastroenterol Hepatol*. 2009;6:228–235.
- Giuffrida P, Biancheri P, MacDonald TT. Proteases and small intestinal barrier function in health and disease. *Curr Opin Gastroenterol*. 2014;30:147–153.
- Marshall NC, Finlay BB, Overall CM. Sharpening host defenses during infection: proteases cut to the chase. *Mol Cell Proteomics*. 2017;16:S161–S171.
- Parks WC, Wilson CL, López-Boado YS. Matrix metalloproteinases as modulators of inflammation and innate immunity. *Nat Rev Immunol*. 2004;4:617–629.
- Morrison CJ, Butler GS, Rodríguez D, et al. Matrix metalloproteinase proteomics: substrates, targets, and therapy. *Curr Opin Cell Biol*. 2009;21:645–653.
- Sorokin L. The impact of the extracellular matrix on inflammation. *Nat Rev Immunol*. 2010;10:712–723.
- Hopps E, Caimi G. Matrix metalloproteinases in metabolic syndrome. *Eur J Intern Med*. 2012;23:99–104.
- Breynaert C, de Bruyn M, Arijis I, et al. Genetic deletion of tissue inhibitor of metalloproteinase-1/TIMP-1 alters inflammation and attenuates fibrosis in dextran sodium sulphate-induced murine models of colitis. *J Crohns Colitis*. 2016;10:1336–1350.
- Di Sabatino A, Jackson CL, Pickard KM, et al. Transforming growth factor beta signalling and matrix metalloproteinases in the mucosa overlying Crohn's disease strictures. *Gut*. 2009;58:777–789.
- Specia S, Giusti I, Rieder F, et al. Cellular and molecular mechanisms of intestinal fibrosis. *World J Gastroenterol*. 2012;18:3635–3661.
- Biancheri P, Giuffrida P, Docena GH, et al. The role of transforming growth factor (TGF)- $\beta$  in modulating the immune response and fibrogenesis in the gut. *Cytokine Growth Factor Rev*. 2014;25:45–55.
- Goffin L, Fagagnini S, Vicari A, et al. Anti-MMP-9 antibody: A promising therapeutic strategy for treatment of inflammatory bowel disease complications with fibrosis. *Inflamm Bowel Dis*. 2016;22:2041–2057.
- Rieder F, Kessler S, Sans M, et al. Animal models of intestinal fibrosis: new tools for the understanding of pathogenesis and therapy of human disease. *Am J Physiol Gastrointest Liver Physiol*. 2012;303:G786–G801.
- Grassl GA, Valdez Y, Bergstrom KS, et al. Chronic enteric salmonella infection in mice leads to severe and persistent intestinal fibrosis. *Gastroenterology*. 2008;134:768–780.
- Månsson LE, Montero M, Zarepour M, et al. MyD88 signaling promotes both mucosal homeostatic and fibrotic responses during *Salmonella*-induced colitis. *Am J Physiol Gastrointest Liver Physiol*. 2012;303:G311–G323.
- Johnson LA, Rodansky ES, Moons DS, et al. Optimisation of intestinal fibrosis and survival in the mouse *S. Typhimurium* model for anti-fibrotic drug discovery and preclinical applications. *J Crohns Colitis*. 2017;11:724–736.
- Lo BC, Gold MJ, Hughes MR, et al. The orphan nuclear receptor ROR $\alpha$  and group 3 innate lymphoid cells drive fibrosis in a mouse model of Crohn's disease. *Sci Immunol*. 2016;1:eaf8864.
- Johnson LA, Luke A, Sauder K, et al. Intestinal fibrosis is reduced by early elimination of inflammation in a mouse model of IBD: impact of a “top-down” approach to intestinal fibrosis in mice. *Inflamm Bowel Dis*. 2012;18:460–471.
- Hoiseh SK, Stocker BA. Aromatic-dependent *Salmonella typhimurium* are non-virulent and effective as live vaccines. *Nature*. 1981;291:238–239.
- Claes AK, Steck N, Schultz D, et al. *Salmonella enterica* serovar Typhimurium AmsbB triggers exacerbated inflammation in Nod2 deficient mice. *PLoS One*. 2014;9:e113645.
- Kappelhoff R, Puente XS, Wilson CH, et al. Overview of transcriptomic analysis of all human proteases, non-proteolytic homologs and inhibitors: organ, tissue and ovarian cancer cell line expression profiling of the human protease degradome by the CLIP-CHIP™ DNA microarray. *Biochim Biophys Acta Mol Cell Res*. 2017;1864:2210–2219.
- Kappelhoff R, Overall C. The CLIP-CHIP oligonucleotide microarray: dedicated array for analysis of all protease, nonproteolytic homolog, and inhibitor gene transcripts in human and mouse. *Curr Protoc Protein Sci*. 2009;Chapter 21:Unit21.19.
- Kappelhoff R, Auf dem Keller U, Overall CM. Analysis of the degradome with the CLIP-CHIP microarray. *Methods Mol Biol*. 2010;622:175–193.
- Tusher VG, Tibshirani R, Chu G. Significance analysis of microarrays applied to the ionizing radiation response. *Proc Natl Acad Sci U S A*. 2001;98:5116–5121.
- de Bruyn M, Vandooren J, Ugarte-Berzal E, et al. The molecular biology of matrix metalloproteinases and tissue inhibitors of metalloproteinases in inflammatory bowel diseases. *Crit Rev Biochem Mol Biol*. 2016;51:295–358.
- Pender SL, Croucher PJ, Mascheretti S, et al. Transmission disequilibrium test of stromelysin-1 gene variation in relation to Crohn's disease. *J Med Genet*. 2004;41:e112.
- Vaalamo M, Karjalainen-Lindsberg ML, Puolakkainen P, et al. Distinct expression profiles of stromelysin-2 (MMP-10), collagenase-3 (MMP-13), macrophage metalloelastase (MMP-12), and tissue inhibitor of metalloproteinases-3 (TIMP-3) in intestinal ulcerations. *Am J Pathol*. 1998;152:1005–1014.
- Eguchi T, Kubota S, Kawata K, et al. Novel transcription-factor-like function of human matrix metalloproteinase 3 regulating the CTGF/CCN2 gene. *Mol Cell Biol*. 2008;28:2391–2413.
- Marchant DJ, Bellac CL, Moraes TJ, et al. A new transcriptional role for matrix metalloproteinase-12 in antiviral immunity. *Nat Med*. 2014;20:493–502.
- Dean RA, Butler GS, Hama-Kourbali Y, et al. Identification of candidate angiogenic inhibitors processed by matrix metalloproteinase 2 (MMP-2) in cell-based proteomic screens: disruption of vascular endothelial growth factor (VEGF)/heparin affinity regulatory peptide (pleiotrophin) and VEGF/connective tissue growth factor angiogenic inhibitory complexes by MMP-2 proteolysis. *Mol Cell Biol*. 2007;27:8454–8465.
- McKaig BC, McWilliams D, Watson SA, et al. Expression and regulation of tissue inhibitor of metalloproteinase-1 and matrix metalloproteinases by intestinal myofibroblasts in inflammatory bowel disease. *Am J Pathol*. 2003;162:1355–1360.
- Graham MF, Diegelmann RF, Elson CO, et al. Collagen content and types in the intestinal strictures of Crohn's disease. *Gastroenterology*. 1988;94:257–265.
- Lawrance IC, Wu F, Leite AZ, et al. A murine model of chronic inflammation-induced intestinal fibrosis down-regulated by antisense NF-kappa B. *Gastroenterology*. 2003;125:1750–1761.
- Kobuch J, Cui H, Grünwald B, et al. TIMP-1 signaling via CD63 triggers granulopoiesis and neutrophilia in mice. *Haematologica*. 2015;100:1005–1013.
- Di Sabatino A, Pender SL, Jackson CL, et al. Functional modulation of Crohn's disease myofibroblasts by anti-tumor necrosis factor antibodies. *Gastroenterology*. 2007;133:137–149.
- Arnold P, Otte A, Becker-Pauly C. Meprin metalloproteases: molecular regulation and function in inflammation and fibrosis. *Biochim Biophys Acta Mol Cell Res*. 2017;1864:2096–2104.
- Banerjee S, Jin G, Bradley SG, et al. Balance of meprin A and B in mice affects the progression of experimental inflammatory bowel disease. *Am J Physiol Gastrointest Liver Physiol*. 2011;300:G273–G282.
- Vazelle E, Bringer MA, Gardarin A, et al. Role of meprins to protect ileal mucosa of Crohn's disease patients from colonization by adherent-invasive *E. Coli*. *PLoS One*. 2011;6:e21199.
- Kirkegaard T, Hansen A, Bruun E, et al. Expression and localisation of matrix metalloproteinases and their natural inhibitors in fistulae of patients with Crohn's disease. *Gut*. 2004;53:701–709.
- Saarialho-Kere UK, Vaalamo M, Puolakkainen P, et al. Enhanced expression of matrilysin, collagenase, and stromelysin-1 in gastrointestinal ulcers. *Am J Pathol*. 1996;148:519–526.

42. Monteleone G, Caruso R, Fina D, et al. Control of matrix metalloproteinase production in human intestinal fibroblasts by interleukin 21. *Gut*. 2006;55:1774–1780.
43. Garg P, Vijay-Kumar M, Wang L, et al. Matrix metalloproteinase-9-mediated tissue injury overrides the protective effect of matrix metalloproteinase-2 during colitis. *Am J Physiol Gastrointest Liver Physiol*. 2009;296:G175–G184.
44. Liu H, Patel NR, Walter L, et al. Constitutive expression of MMP9 in intestinal epithelium worsens murine acute colitis and is associated with increased levels of proinflammatory cytokine Kc. *Am J Physiol Gastrointest Liver Physiol*. 2013;304:G793–G803.
45. Loftus EV Jr. Clinical epidemiology of inflammatory bowel disease: incidence, prevalence, and environmental influences. *Gastroenterology*. 2004;126:1504–1517.
46. Darfeuille-Michaud A, Boudeau J, Bulois P, et al. High prevalence of adherent-invasive *Escherichia coli* associated with ileal mucosa in Crohn's disease. *Gastroenterology*. 2004;127:412–421.
47. Gradel KO, Nielsen HL, Schönheyder HC, et al. Increased short- and long-term risk of inflammatory bowel disease after salmonella or campylobacter gastroenteritis. *Gastroenterology*. 2009;137:495–501.
48. Lu R, Bosland M, Xia Y, et al. Presence of *Salmonella avra* in colorectal tumor and its precursor lesions in mouse intestine and human specimens. *Oncotarget*. 2017;8:55104–55115.
49. Nazareth N, Magro F, Machado E, et al. Prevalence of *Mycobacterium avium* subsp. Paratuberculosis and *Escherichia coli* in blood samples from patients with inflammatory bowel disease. *Med Microbiol Immunol*. 2015;204:681–692.
50. Bosca-Watts MM, Tosca J, Anton R, et al. Pathogenesis of Crohn's disease: bug or no bug. *World J Gastrointest Pathophysiol*. 2015;6:1–12.
51. Jess T, Simonsen J, Nielsen NM, et al. Enteric salmonella or campylobacter infections and the risk of inflammatory bowel disease. *Gut*. 2011;60:318–324.
52. Riddle MS, Porter CK. Detection bias and the association between inflammatory bowel disease and salmonella and campylobacter infection. *Gut*. 2012;61:635.
53. García Rodríguez LA, Ruigómez A, Panés J. Acute gastroenteritis is followed by an increased risk of inflammatory bowel disease. *Gastroenterology*. 2006;130:1588–1594.
54. Vergnolle N. Protease inhibition as new therapeutic strategy for GI diseases. *Gut*. 2016;65:1215–1224.